Assessment of conductor thermal models for grid studies

J.R. Santos, A. Gómez Expósito and F. Parreño Sánchez

Abstract: Existing EMS applications resort to static network models built upon constant resistances whose values are specified beforehand. However, the steady-state thermal balance of overhead conductors requires that ohmic losses be dissipated by convection and radiation heat, leading to conductor resistances being a function both of environmental factors and transmitted current. Each term of the equation involved in the thermal balance of overhead conductors is analysed allowing the influence of conductor current on conductor temperature to be separated from that corresponding to environmental factors. As a result, three approximate thermal models are elaborated, which are compared on the Spanish transmission system. Test cases are included showing that the influence of the selected model on transmission losses may be significant enough, particularly when the transmission system spans areas with diverse loading levels and weather conditions.

1 Introduction

Currents flowing through overhead conductors give rise to Joule losses that raise their temperature. Besides the amount of ohmic losses dissipated, several environmental factors (mainly ambient temperature and wind speed) and conductor parameters (diameter and emissivity) determine the equilibrium temperature reached by the conductor. It is well-known that the resistance of a metallic wire grows almost linearly with its temperature. Therefore, strictly speaking, transmission lines are not linear time-invariant components as their resistance is a function of both time and current. As a matter of fact, differences between summer and winter line resistances over 15% have been reported [1].

While the dynamic thermal behaviour of individual conductors has been historically the focus of much attention, mainly in ampacity-related studies [2–6], its implications for systemwide studies have been largely neglected. This may be partly due to the fact that something apparently as simple as gathering the correct line parameters for a large transmission system frequently constitutes a cumbersome task, especially if second-order effects are to be considered. Consequently it is customary to adopt a static model when performing routine network studies [7–9] (load flow, state estimation, etc.) in which constant conductor temperatures are assumed throughout, irrespective of the ambient temperature and transmitted power. Typically databases and input files provide line resistances at 20°C.

This paper focuses on the influence of environmental factors and daily load evolution on conductor resistances and, as a consequence, on the results provided by EMS applications, specially regarding transmission power losses. From an analysis of the relative importance of convection and radiation heats, three approximate conductor thermal models are elaborated and compared. For those cases in which conductor temperatures are not measured, a simple methodology based on repeated load-flow solutions is adopted to obtain more accurate values of line resistances. Test cases show that noticeable modifications in transmission power losses occur when resistances corresponding to estimated conductor temperatures are employed rather than constant resistances. The economic importance of such discrepancies may not be negligible in nowadays liberalised markets [10].

2 Thermal balance of overhead conductors

As ambient temperature and power demand fluctuate slowly enough, it can be assumed in practice that overhead conductors are in steady state, both from the electrical and thermal points of view. In consequence, the following thermal balance equation applies [6, 11, 12]:

$$Q_j + Q_s = Q_r + Q_c \quad [\text{W/m}] \tag{1}$$

where

Q_j: Joule losses

Q_s: heat absorbed by solar radiation

Q_r: radiative heat transfer

Q_c: convective heat transfer.

Joule losses are computed from

$$Q_j = I^2 R_c \quad [\text{W/m}] \tag{2}$$

where I is the conductor current (A) and R_c the unitary resistance (Ω/m) at conductor temperature T_c (°C). In turn, the conductor resistance is a function of temperature, as follows:

$$R_c = R_0[1 + \alpha(T_c - T_0)] \tag{3}$$

where

T_0: reference temperature (°C)

IET Gener. Transm. Distrib., Vol. 1, No. 1, January 2007

155

R_0: conductor resistance at temperature T_0 (Ω/m)

α: temperature coefficient of resistance at temperature T_0 ($^\circ C^{-1}$).

The coefficient α is somewhat affected by temperature, but this dependence is customarily ignored. This allows writing expressions like (3) for different temperatures, which can be considered exact for practical purposes. Of particular interest for this paper is the following one:

$$R_c = R_a[1 + \alpha(T_c - T_a)] \qquad (4)$$

where

T_a: ambient temperature ($^\circ$C)

R_a: conductor resistance at temperature T_a (Ω/m).

The conductor is also heated by solar radiation, given by

$$Q_s = W_s d_c \quad [\text{W/m}] \qquad (5)$$

where W_s is the incident solar energy (W/m^2) and d_c the conductor diameter (m).

On the other hand, convection and radiation heat emission can be accurately computed by means of well-known empirical expressions [6, 12]

$$Q_c = S \frac{5.727\sqrt{pv}}{(T_a + 273.15)^{0.123}\sqrt{d_c}}(T_c - T_a) \quad [\text{W/m}] \qquad (6)$$

$$Q_r = 17.8204 E d_c \left[\left(\frac{T_c + 273.15}{100}\right)^4 \left(\frac{T_a + 273.15}{100}\right)^4\right] \quad [\text{W/m}] \qquad (7)$$
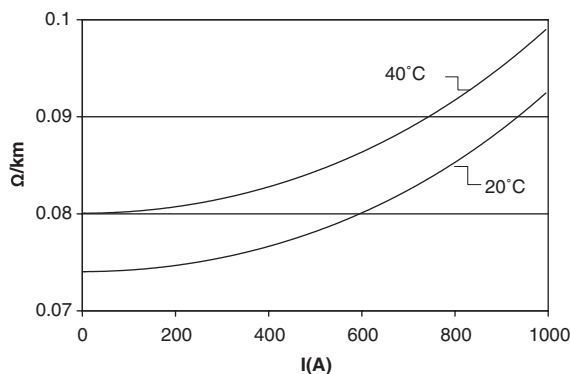
where

S: conductor surface (m^2/m)

p: atmospheric pressure (atm)

v: wind speed (m/s)

E: emissivity constant.

Equation (6) ignores the natural convective heat transfer, whose relative importance diminishes rapidly as the wind velocity increases. For $d_c = 0.02$ m and $T_c - T_a = 50^\circ$C, the resulting error by ignoring natural convection falls to 1% when $v \geq 0.53$ m/s [13]. However, when the wind velocity is low, the additional heat transfer due to natural convection should be taken into account. For instance, when $v = 0.1$ m/s the calculated total heat transfer is up to 30% higher than that based on pure forced convection [6, 11].

When (2)–(7) are substituted into (1) a nonlinear expression is obtained allowing the conductor temperature to be computed for a given conductor current and weather conditions (ambient temperature and pressure, wind speed and solar radiation), that is

$$T_c = f(I, T_a, p, v, W_s) \qquad (8)$$

Once T_c is computed, the exact value for the conductor resistance R_c can be obtained from (3).

Figure 1 shows the steady-state temperature reached by a Condor conductor (LA455) as a function of the ambient temperature ($p = 1$ atm, $v = 0.6$ m/s, $E = 0.5$, $W_s = 375$ W/m^2) for different conductor currents. As proved in the Appendix (Section 8.1), the difference between conductor and ambient temperatures is nearly constant for a given current, which explains the linear relationship with unity slope shown in the Figure.

For the same conductor, Fig. 2 (left) represents its resistance against transmitted current for two ambient temperatures (same environmental conditions). As clearly noticed, the conductor resistance increases more than linearly with conductor current (Section 8.1). This translates into Joule losses growing more than quadratically with conductor current, as illustrated in Fig. 2 (right) where the constant resistance case (quadratic losses) is included for comparison.

As discussed in Section 8.1, for the conductor temperatures typically found in practice ($T_c < 80^\circ$C), heat evacuation by radiation can be approximately expressed as a linear function of $T_c - T_a$ (see Fig. 3). This simplification leads to the following relationship:

$$R_c = \beta R_a \qquad (9)$$

where β is essentially a function of conductor current and wind speed. Figure 4 represents this dependence for a
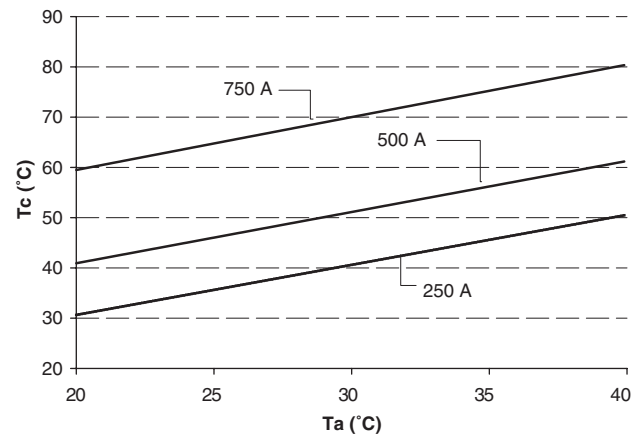

Fig. 1 *Steady-state Condor conductor temperature against ambient temperature for different currents*
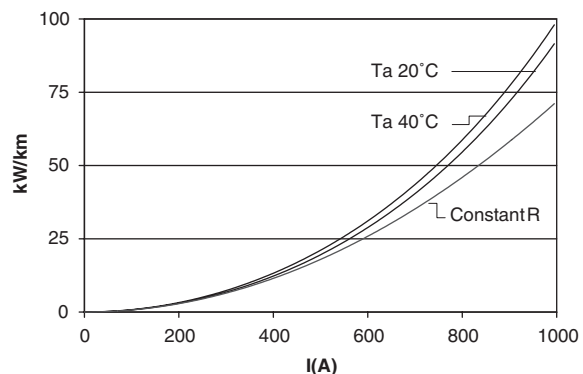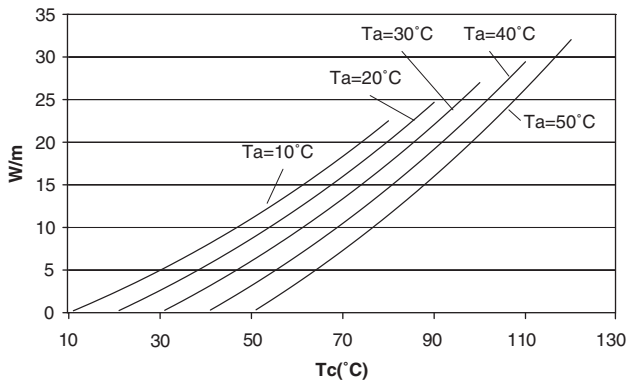

Fig. 2 *Condor conductor resistance and ohmic losses against transmitted current*

156

IET Gener. Transm. Distrib., Vol. 1, No. 1, January 2007

Fig. 3 *Radiative heat transfer against Condor conductor temperature for different ambient temperatures*
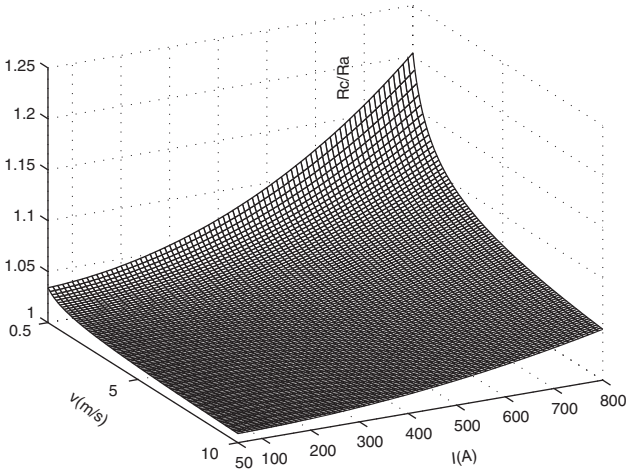
Fig. 4 *Parameter β against conductor current and wind speed*

Table 1: Components of the thermal balance equation for typical summer conditions under peak load in Spain

Voltage (kV)	Type	d_c (mm)	Q_c [W/m]	Q_r [W/m]	Q_s [W/m]	$(Q_r - Q_s)/Q_c$ (%)
132	LA380	25.38	55.2	14.648	9.518	9.3
220	LA455	27.72	57.69	15.998	10.395	9.7
400	LA545	30.42	60.43	17.55	11.408	10.2

Condor conductor ($T_a = 20°C$, $W_s = 375\,W/m^2$). Note that, for small wind speeds and large currents, β can be as large as 1.20, which translates into Joule losses being underestimated by 20% if R_a instead of R_c is used.

Table 1 shows, for the set of conductors typically employed at transmission levels and average summer environmental conditions in Spain ($p = 1\,atm$, $v = 0.6\,m/s$, $W_s = 375\,W/m^2$, $T_a = 20°C$ and $E = 0.5$) the relative importance of each term in (1) assuming the conductor current is of such magnitude that $T_c = 70°C$. Even though Q_r is not negligible compared to Q_c, it is worth noting that, for the particular operating point considered in the Table, Q_r cancels out Q_s to a large extent. As shown in the rightmost column, the error arising by ignoring both Q_r and Q_s is around 10% in this case.

3 Approximate conductor resistance models

In this paper the exact model derived will be compared with approximate simpler models which are or can be employed in network-related studies.

The customary model adopted for steady-state grid analysis (load flows, congestion assessment, power loss allocation, etc.) is the one that computes all conductor resistances at a fixed reference temperature (usually $T_0 = 20°C$).

An alternative model consists of assuming that conductor temperatures do not differ significantly from ambient temperatures, which is equivalent to setting $\beta = 1$ in (9). As getting the exact ambient temperature distribution along each line is not viable, the simplified averaging technique developed in Section 8.2, based on the assumption that temperatures evolve linearly between two points, should be adopted in practice. Nowadays the required local information can be obtained online through the internet from weather forecasting services.

The most accurate model is the one based on actual conductor temperatures, which can be measured at certain points and collected through the SCADA system. This is a possibility currently offered by several SCADA vendors in their catalogues [14]. Like in the former model, the averaging procedure described in Section 8.2 should be resorted to, as it is impossible to locally measure the temperature along the whole conductor length.

When conductor temperatures are not measured they can be alternatively obtained by solving (8) for a set of weather conditions and a given conductor current. In fact, this is the only procedure that can be applied until new generations of SCADA systems, providing conductor temperatures, become a reality. However, as conductor currents are unknown in advance the solution of (8) must be somehow combined with that of a conventional load flow, for which the iterative procedure described in Section 8.3 can be employed.

To assess the accuracy of the three models, (3) is rearranged as follows:

$$R_c = R_0[1 + \alpha(T_c - T_a) + \alpha(T_a - T_0)] \quad (10)$$

allowing the total resistance error

$$\varepsilon_R = \frac{R_c - R_0}{R_0} \quad (11)$$

to be split into the following two terms:

$$\varepsilon_R = \alpha(T_c - T_a) + \alpha(T_a - T_0) = \varepsilon_{ca} + \varepsilon_{a0} \quad (12)$$

The nonnegative error component ε_{ca} is due to the conductor temperature raise over ambient temperature, and can be related with the parameter β as

$$\varepsilon_{ca} = \beta - 1 \quad (13)$$

Ignoring conductor heating by solar radiation ($W_s \approx 0$) this component is clearly null for steady-state unloaded conductors ($I = 0$). Therefore, as a first approximation, it can be solely attributed to the circulation of current, its importance being relatively high for congested lines (see the representation of β in Fig. 4).

On the other hand, the error component ε_{a0} can be positive or negative, depending on the local temperature. If T_0 is appropriately chosen to represent the average regional temperature, and different input files are prepared for each season, the effect of this component should not be very important. However, as will be shown by the following experimental results, it is not necessarily negligible for transmission networks spanning large geographical areas, where temperature differences as large as $20°C$ are possible.

In summary, the following three models are considered:

M_0: conductor resistances computed at a fixed arbitrary temperature T_0

M_a: conductor resistances computed at given ambient temperatures T_a

M_c: conductor resistances computed at conductor temperatures T_c.

In turn, two possibilities can be considered for model M_c, namely:

M_{cm}: conductor temperature is locally measured and received via SCADA from remote terminal units

M_{ce}: conductor temperature is estimated for an assumed set of weather conditions and conductor current, by solving (8). To obtain conductor currents the iterative procedure described in Section 8.3 can be adopted.

As new and more sophisticated generations of SCADA systems become common, model M_{cm} will gain wider acceptance as a way of more accurately monitoring potential congestions, transmission losses, etc.

4 Experimental results

The Spanish transmission system is tested on a representative summer day to illustrate potential discrepancies among the three conductor thermal models presented. The test system comprises 731 buses and 1064 lines (including double circuits), spanning the three transmission levels existing in Spain (400, 220 and 132 kV). Depending on the voltage level the conductor types shown in Table 1 are selected, the conductor arrangement (simplex or duplex conductor) being a function of the transmitted power. Figure 5 represents the aggregated load evolution that took place on the test day (taken from [15]).

According to average data corresponding to the summer season in Spain, the incident solar energy W_s has been chosen as follows:

- $W_s = 0$ from 22:00 to 7:00.
- W_s increases linearly from 0 to 375 W/m^2 between 7:00 and 15:00.
- $W_s = 375$ W/m^2 from 15:00 to 17:00.
- W_s decreases linearly from 375 W/m^2 to 0 between 17:00 and 22:00.

So far as ambient temperature distribution is concerned, only five areas are considered for simplicity, as shown in Fig. 6 (in all cases, $p = 1$ atm, $v = 0.6$ m/s, $E = 0.5$). In addition, Portugal and the South of France constitute external areas interconnected to the Spanish system by several lines. Temperatures at all substations within an area
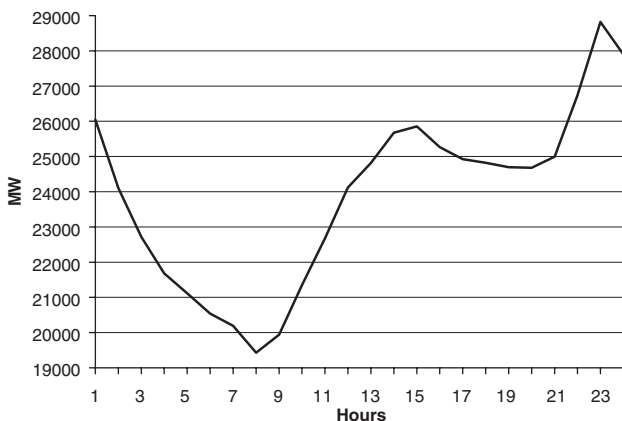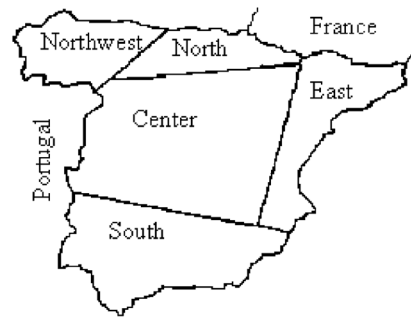

Fig. 6 *Areas where temperatures are assumed to be uniform*
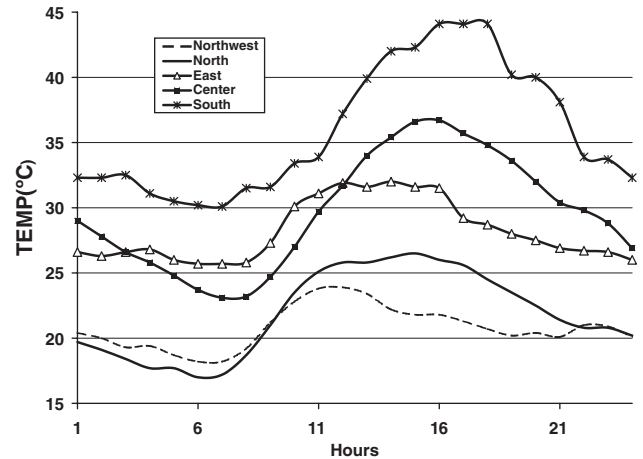

Fig. 7 *Daily evolution of temperatures at representative places*

are assumed to be the same as that of a representative place, selected on the basis of weather records.

The actual hourly temperature evolution that took place at the five chosen places on the test day is shown in Fig. 7. Note the significant temperature differences between the Southern and Northern areas throughout the day, the Central area lying in between (the temperatures corresponding to France and Portugal are assumed for simplicity to be equal to the Northern and the average between the Central and Southern areas, respectively). For lines whose terminal buses belong to different areas the average temperature value is adopted, according to Section 8.2.
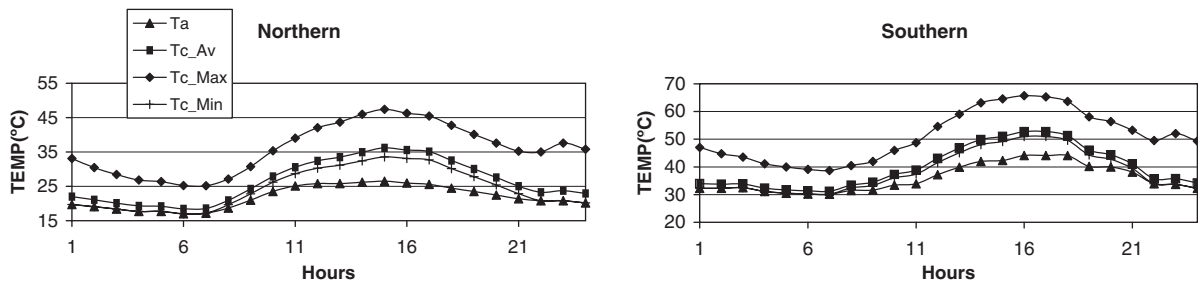
Three scenarios, corresponding respectively to models M_0, M_a and M_c have been simulated and analysed, namely:

A: Conventional load-flow solution with constant conductor temperature ($T_0 = 20$°C is adopted).

B: Load-flow solution with conductor temperature equal to ambient temperature (as given by Fig. 7).

C: Iterated solution of the load flow and (8), to estimate average conductor temperatures (Section 8.3). This corresponds to model M_{ce}, but could be replaced by model M_{cm} if actual conductor temperatures were provided by remote terminal units.

When solving (8) to obtain conductor temperatures the major sources of errors are related with wind speed, which is assumed constant throughout the country, and ambient temperature, assumed constant throughout each region. Indeed, considering exact environmental conditions for each kilometre of line, including not only wind speed but also wind direction, would be nearly impossible, which is the reason why the use of model M_{cm} is advocated.

Figure 8 represents, for the Northern and Southern areas respectively, the daily evolution of the ambient temperature,

Fig. 5 *Aggregated demand for Spanish system on July 25, 2004*

158

IET Gener. Transm. Distrib., Vol. 1, No. 1, January 2007

Fig. 8 *Daily evolution of ambient and conductor temperatures in Northern and Southern regions*

along with the average conductor temperature and the minimum and maximum temperatures reached by any conductor in those regions, according to the results provided by model M_{ce}. Note that during valley or low load conditions average conductor temperatures are very close to ambient temperatures, as expected. At peak hours (13:00–17:00) the minimum and maximum conductor temperatures are respectively around 7 and 20°C higher than that of the ambient. On the other hand, during the evening peak (23:00), conductor temperatures are not so high owing to the decreasing ambient temperatures.

All of these findings, along with a careful analysis of the remaining results provided by model M_{ce}, confirm that this simplified model is accurate enough for the purposes of this paper. In other words, the conductor temperatures obtained by simulation correspond with feasible and realistic operating points for the typical summertime in Spain. Therefore, in the absence of more accurate information, it is assumed in the sequel that scenario C reflects actual operating conditions.

Figure 9 represents the system power losses obtained for the three scenarios considered.

Taking as a reference the values corresponding to the conventional load-flow solution (scenario A), the total relative error associated with power losses, given by

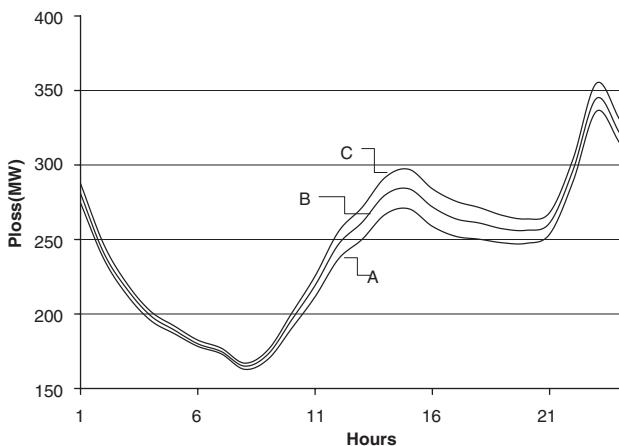$$\varepsilon_{tot} = [P_{loss}(C) - P_{loss}(A)]/P_{loss}(A)$$

can be split as

$$\varepsilon_{tot} = \varepsilon_W + \varepsilon_I$$

where

$$\varepsilon_I = [P_{loss}(C) - P_{loss}(B)]/P_{loss}(A)$$
$$\varepsilon_W = [P_{loss}(B) - P_{loss}(A)]/P_{loss}(A)$$

As discussed, the differences in load-flow solution and losses between cases B and C, represented by ε_I, arise because of the dependence of the conductor temperature on its own current (in the absence of current the conductor and ambient temperatures would be nearly the same in steady state). On the other hand, the discrepancies between cases A and B (ε_W) are due to the temperature gradient.

Figure 10 (upper left) represents the hourly evolution of the three error components defined. Note that such errors are slightly different from those given by (12), owing to minor differences in conductor currents among the three scenarios. The largest total error, close to 10%, takes place during the afternoon peak. In absolute terms, the total error throughout the day translates into 344 MWh of difference between cases A and C.

It is also interesting to analyse how the power-loss computation errors split by areas. Figure 10 (upper right) shows that, unlike the total system error which is always positive for the tested day, the resulting error corresponding to the Northwestern area is negative. Also, relative errors much larger than the average can be noticed for certain areas (over 20% reaching a 30% peak for the Central area).

The two lower diagrams of Fig. 10 represent the current and weather components of the relative errors by areas. It can be observed that

- In the South, where summer temperatures are extreme, errors due to weather conditions are more significant than those arising from conductor loading.

- In the Central area, where the capital is located and branch power flows tend to be comparatively larger, errors due to transmitted power are noticeably higher than in other areas, and remain essentially constant throughout the day.

- In the Northwest, where ambient temperature is closer to T_0, the error component ε_W is less relevant than ε_I.

5 Conclusions

Overhead conductor temperatures can be in practice significantly affected by transmitted power and weather conditions. This effect is customarily ignored by conventional load-flow solvers and other EMS tools, as they resort to databases in which conductor resistances are specified beforehand for a certain typical temperature. In this paper, the influence of conductor current and weather conditions on the conductor resistance has been separately analysed. This leads to two approximate conductor thermal models which are subsequently compared with the exact model based on actual conductor temperatures. As conductor temperatures are not yet available in most EMS, an iterative procedure involving a conventional load flow is proposed to estimate average conductor temperatures. Test cases corresponding to the Spanish transmission network, comprising areas with diverse loading levels and weather
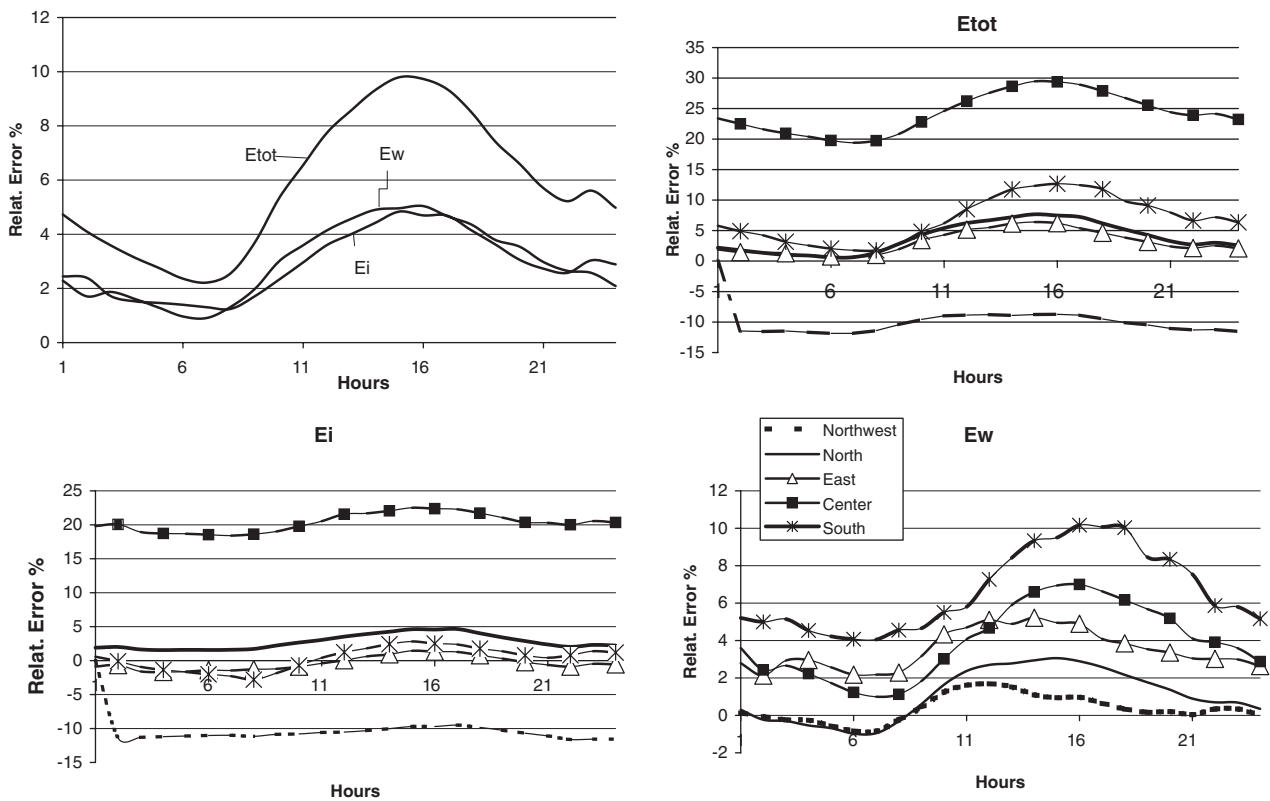

Fig. 9 *Daily evolution of system power losses for three scenarios simulated*

IET Gener. Transm. Distrib., Vol. 1, No. 1, January 2007

159

Fig. 10 *Relative error components of power losses (upper left) and disaggregation by areas*

conditions, are included showing that the influence of conductor temperatures on transmission losses is not negligible. For a typical summer day errors in transmission losses are close to 10% under peak loading for the whole system, and they can almost reach 30% when certain areas are individually considered. Agents participating in nowadays liberalised markets should be aware of these potential discrepancies, which can be easily assessed by adopting the methodology developed in this paper.

6 Acknowledgment

7 References

1 'Electrical transmission and distribution reference book' (Westinghouse Electric, 1942)
2 Morgan, V.T.: 'Thermal behaviour of electrical conductors' (Research Studies Press, John Wiley, New York, 1991)
3 Douglas, D.A., and Edris, A.A.: 'Real-time monitoring and dynamic thermal rating of power transmission circuits', *IEEE Trans. Power Deliv.*, 1996, **11**, (3), pp. 1407–1417
4 Foss, S.D., Lin, S.H., and Fernández, R.A.: 'Dynamic thermal line ratings. Part I: Dynamic ampacity algorithm', *IEEE Trans. Power Appar. Syst.*, 1983, pp. 1858–1864
5 Anders, G.J., and Brakelmann, H.: 'Improvement in cable rating calculations by consideration of dependence of losses on temperature', *IEEE Trans. Power Deliv.*, 2004, **19**, (3), pp. 919–925
6 IEEE Standard 738–1993: 'Calculating the current-temperature relationship of bare overhead conductors' Nov. 1993
7 Tinney, W.F., and Hart, C.E.: 'Power-flow solution by Newton's method', *IEEE Trans. Power Appar. Syst.*, 1967, **PAS-86**, pp. 1449–1460
8 Stott, B.: 'Review of load flow calculation methods', *Proc. IEEE*, 1974, **62**, (7), pp. 916–929
9 Abur, A., and Gómez, A.: 'Power system state estimation. Theory and implementation' (Marcel Dekker, New York, 2004)
10 Banakar, H., Alguacil, N., and Galiana, F.D.: 'Electrothermal coordination. Part I: Theory and implementation schemes', *IEEE Trans. Power Syst.*, 2005, **20**, (2), pp. 798–805
11 CIGRE CE/SC22, 'Thermal behaviour of overhead conductors', Technical Brochure 207, 2002
12 'The electric power engineering handbook' (Ed. CRC Press and IEEE Press)
13 Morgan, V.T.: 'Effect of mixed convection on the external thermal resistance of single-core and multicore bundled cables in air', *IEE Proc.-C*, 1992, **139**, (2), pp. 109–116
14 InformIT Wide Area Monitoring PSG 850 ABB
15 www.ree.es
16 Black, W.Z., and Rehberg, R.L.: 'Simplified model for steady-state and real-time ampacity of overhead conductors'. Presented at the IEEE/PES Winter Meeting, Paper 88 WM 236-5, 1985
17 Callahan, P.M., and Douglass, D.A.: 'An experimental evaluation of a thermal line uprating by conductor temperature and weather monitoring', *IEEE Trans. Power Syst.*, 1988, **3**, (4), pp. 1960–1967

8 Appendix

8.1 Simplifications to thermal balance equation

A simplified thermal balance equation is developed which explains the shape of the functions shown in Figs. 1 and 2.

According to [16, 17], for normal operating conditions, the radiation heat term Q_r in (1), can be roughly approximated as a linear function of the conductor temperature rise above ambient ($T_c - T_a$). Therefore

$$Q_r \cong K_r(T_c - T_a) \qquad (14)$$

where the constant K_r is computed for a given T_a. This nearly linear relationship is shown in Fig. 3 for the Condor conductor.

Now, focus on the convection heat Q_c. For ambient temperatures ranging between -15 and $50°C$, the term $(T_a + 273.15)^{0.123}$ in the denominator of (6) varies between 1.98 and 2.04. Therefore it is reasonable to assume that $(T_a + 273.15)^{0.123} \approx 2$. For $p = 1\,atm$, this simplification leads to

$$Q_c = K_c(T_c - T_a) \qquad (15)$$

160

IET Gener. Transm. Distrib., Vol. 1, No. 1, January 2007

where the constant K_c is given by

$$K_c = 2.8636S\sqrt{\frac{v}{d_c}}$$

Substituting (14) and (15) into (1), and taking into account (4), yields

$$W_s d_c + I^2 R_a[1 + \alpha(T_c - T_a)] = K_c(T_c - T_a) + K_r(T_c - T_a) \tag{16}$$

and, rearranging terms,

$$T_c - T_a = \frac{I^2 R_a + W_s d_c}{K - \alpha I^2 R_a} \tag{17}$$

with $K = K_c + K_r$. This expression shows that, for a given current, wind speed and solar radiation, the difference between the conductor and ambient temperatures is constant (Fig. 1). Also, for a given ambient temperature, the conductor temperature, and hence its resistance, is nearly a quadratic function of its current (Fig. 2), as a consequence of the term $\alpha I^2 R_a$ being typically much smaller than K.

Substituting (17) into (4) yields

$$R_c = R_a \frac{K + \alpha W_s d_c}{K - \alpha I^2 R_a} \tag{18}$$

or, in compact form,

$$R_c = R_a \beta \tag{19}$$

In other words, the actual conductor resistance can be obtained as the resistance at ambient temperature times a parameter $\beta \geq 1$, which depends upon weather conditions and circulating current, as shown in Fig. 4.

8.2 Averaging long line resistances

As shown in Fig. 1, when the ambient temperature along a line is not constant, the conductor temperature is subject to the same gradient, which should be taken into account for long lines traversing heterogeneous areas. Although in theory the geographical distribution of temperatures should be fully specified, in practice it is reasonably accurate to assume that the ambient (and hence conductor) temperature along the line evolves linearly between the temperature values of its terminal substations. Hence, for a line between points A and B, where the conductor temperatures are T_A and T_B respectively, the conductor temperature at distance x from A is given by

$$T(x) = T_A + \frac{T_B - T_A}{L}x \tag{20}$$

where L is the line length. Then the resistance per unit of length will be

$$R(x) = R_0[1 + \alpha(T(x) - T_0)] \qquad [\Omega/\text{m}] \tag{21}$$

and the total line resistance

$$\begin{aligned}
R_{AB} &= \int_A^B R(x)dx = \left[R_0 \int_A^B dx + \alpha \int_A^B T(x)dx - \alpha T_0 \int_A^B dx \right] \\
&= R_0 L[1 + \alpha(T_A - T_0) + \alpha(T_B - T_A)/2] \\
&= R_0 L \left[1 + \alpha \left(\frac{T_A + T_B}{2} - T_0 \right) \right] = \frac{R_A + R_B}{2} \quad [\Omega]
\end{aligned} \tag{22}$$

Therefore the line resistance is obtained as the average of the two resistance values obtained as if the whole conductor were at temperatures T_A and T_B, measured at substations A and B. If deemed necessary, a very long line could be divided into several sections so that the application of the above expression to each resulting section is accurate enough, provided temperature information is available at intermediate points.

8.3 Modified load-flow analysis

Computing the load-flow solution, and hence transmission losses, requires obviously that conductor resistances be specified. However, as proved, such resistances are non-linear functions of the respective currents whose values are not known in advance for meshed grids. Therefore some kind of modified load flow analysis is needed, unless conductor temperatures, and hence resistances, are specified in the input data.

For this purpose standard load-flow tools can be embedded within the following iterative procedure:

(i) Line resistances in the input file are set to an initial value, e.g. the one corresponding with $T_c = 20°C$.

(ii) A conventional load-flow solver is run with constant conductor resistances. This yields the line currents.

(iii) Based on those currents, considering local weather conditions specified for each line, conductor temperatures are estimated by solving (8). In the absence of very accurate information, ambient temperature and hence conductor temperature can be assumed to vary linearly between the temperatures at terminal substations.

(iv) Line resistances are updated. If no significant changes in line resistances are observed, then stop. Otherwise, go to step (ii).

At the end of the process, in addition to the load-flow solution, the average conductor temperature for each line, and hence its resistance and associated ohmic losses are obtained. Applying the proposed methodology to other analytical tools, such as state estimators, is straightforward.

IET Gener. Transm. Distrib., Vol. 1, No. 1, January 2007

161